Electronic Supplementary Material (ESI) for Journal of Materials Chemistry A.

Electronic Supplementary Information

High-Efficiency Bubbles Transportation in Aqueous Environment on Serial-Wedge-Shaped Wettability Pattern

Jinlong Song,[#a] Ziai Liu,[#a] Xuyue Wang,[a] Hong Liu,[b] Yao Lu,[c] Xu Deng,[d] Claire J. Carmalt,[e] and Ivan P. Parkin[e]

[a] *Key Laboratory for Precision and Non-traditional Machining Technology of the Ministry of Education, Dalian University of Technology, Dalian 116024, P. R. China.*

[b] *Key Laboratory of Theoretical Chemistry of Environment Ministry of Education, South China Normal University, Guangzhou 510006, P. R. China. Email: hongliu@m.scnu.edu.cn*

[c] *Department of Mechanical Engineering, University College London, London, WC1E 7JE, UK.*

[d] *Institute of Fundamental and Frontier Sciences, University of Electronic Science and Technology of China, Chengdu 610054, P. R. China.*

[e] *Department of Chemistry, University College London, 20 Gordon Street, London, WC1H 0AJ, UK.*

[#] Contribute equally

Table S1 Characterization of the superhydrophobic region and subaqueous superaerophobic region

	Superhydrophobic region (5 μL water droplet)	Superaerophobic region (2 μL air bubble)
Contact angle	159.0±2.3°	155.0±2.8°
Sliding angle	3.1±0.2°	1.3±0.6°
Advancing contact angle	165.0±2.6°	161.0±2.3°
Receding contact angle	152.0±1.2°	151.0±2.4°

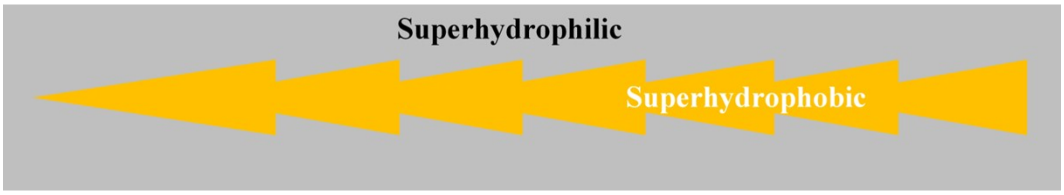

Fig. S1 The schematics of the serial-wedge-shaped wettability pattern with the exterior surrounding superhydrophilic (subaqueous superaerophobic) region and the inside interior superhydrophobic (subaqueous superaerophilic) region. Several single-wedge-shaped patterns were connected end to end (a front triangle and several rear trapezoids with same size and shape), showing that the terminal size has no relationship with the length of the whole pattern.

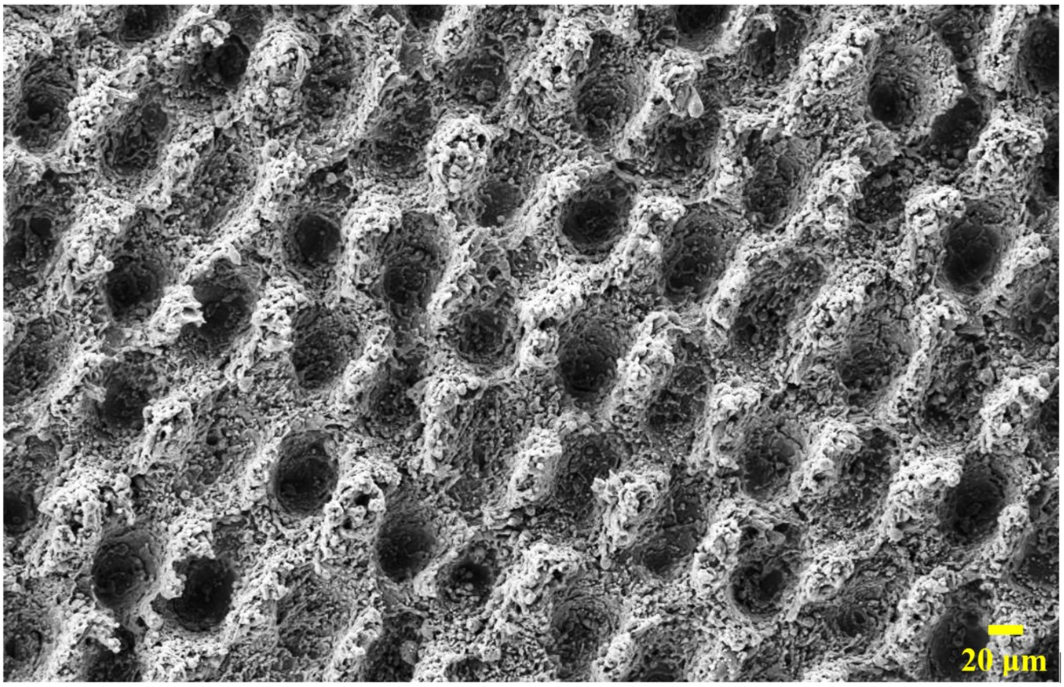

Fig. S2 SEM image of the laser-etched region which shows superhydrophilic. The whole micro morphology was composed of micrometer-scale pores of size 40 μm with protrusions of size 20 μm.

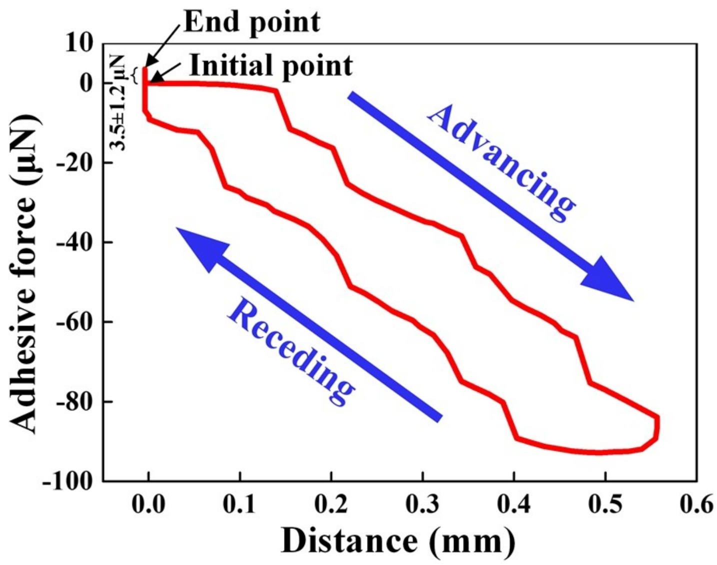

Fig. S3 The adhesive force of a gas bubble with volume of 2 μL on the subaqueous superaerophobic region was measured using an optical contact angle meter (Krüss, DSA100, Germany) integrated with microelectromechanical balance system (Metter A60, Germany). Firstly, gas bubble was suspended on a syringe needle in the water. Before moving the bubble to the superaerophobic surface, the force of the balance system was set to zero. Subsequently, the gas bubble was brought into contact with the superaerophobic surface at a velocity of 0.05 mm/s (Advancing process) and the balance force decreased. When the bubble was detached from the superaerophobic surface at a velocity of 0.05 mm/s, the balance force increased gradually (Receding process). Finally, the bubble broke away from the superaerophobic surface and the balance force reached a critical force which was larger than zero. The critical force (3.5±1.2 μN) to which the gas bubble was subjected can be regarded as the adhesive force between the gas bubble and the superaerophobic surface.

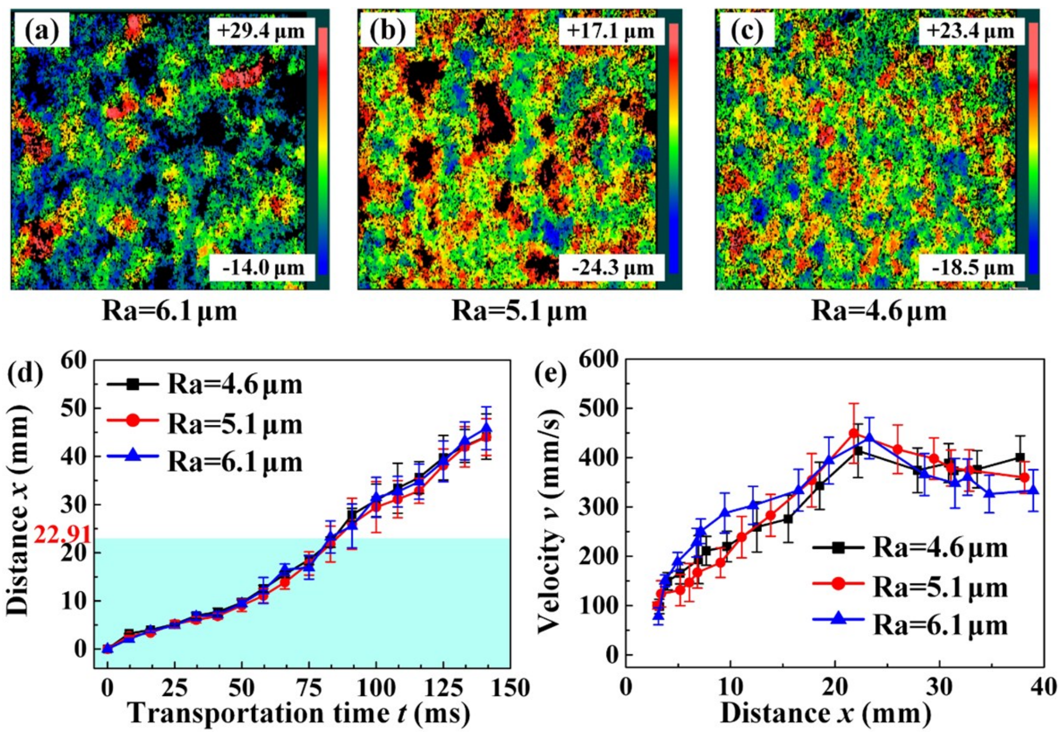

Fig. S4 The effect of the surface roughness on the transportation behavior of gas bubbles. Bubbles were transported on three serial-wedge-shaped wettability patterns with the same geometric parameters (α=4°, w_1=1.2 mm, w_2=2 mm) but different surface roughness (Ra; Ra_1=6.1 μm, Ra_2=5.1 μm, Ra_3=4.6 μm). To prepare three surfaces with different surface roughness, the aluminium plates were electrochemically etched in 0.1 mol/L aqueous sodium chloride (NaCl) solution at 500 mA/cm^2 current density for 5min, 10 min and 15 min, respectively. (a~c) Three superaerophilic surfaces with different surface roughness. (d) The relationship between the transportation distance and transportation time at different surface roughness. (e) The relationship between the transportation velocity and transportation distance at different surface roughness.

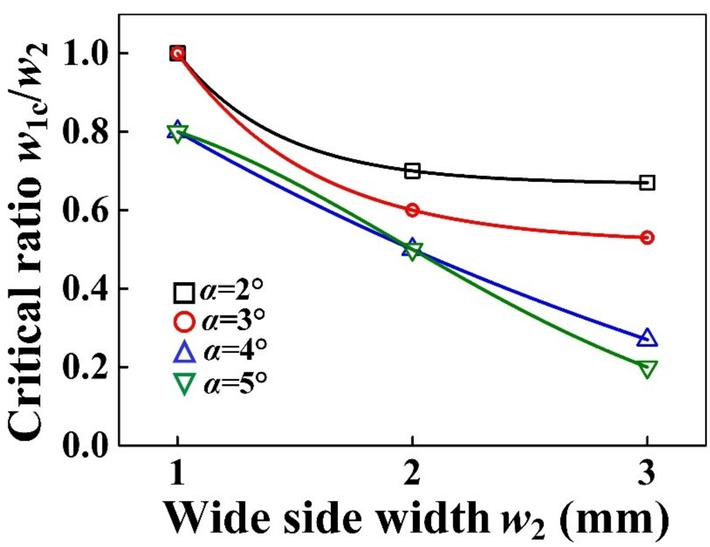

Fig. S5 The relationship between w_{1c}/w_2 and w_2 at different α. For α=2 °, the corresponding curve-fit is $\frac{w_{1c}}{w_2} = -0.67 + 3.33e^{-0.23w_2}$. For α=3 °, the corresponding curve-fit is $\frac{w_{1c}}{w_2} = -0.52 + 2.77e^{-1.7w_2}$. For α=5 °, the corresponding curve-fit is $\frac{w_{1c}}{w_2} = e^{-0.2+0.2w_2-0.22w_2^2}$.

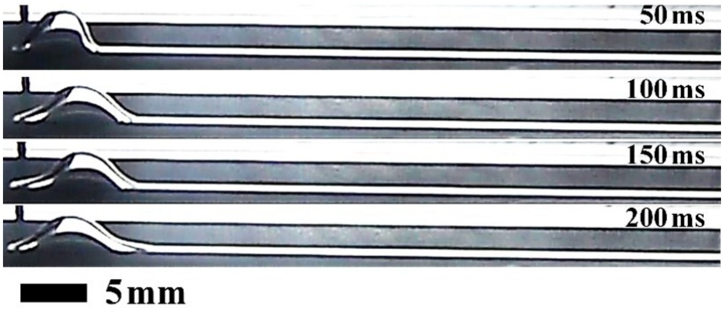

Fig. S6 The transportation processes of a subaqueous gas bubble with volume of 40 μL on a rectangle wettability pattern with a constant width of 2 mm. Once contacted with the left side of the rectangle wettability pattern, the gas bubble was immediately captured. However, owing to the lack of geometric gradient, the rectangle wettability pattern did not have the capacity of transporting the gas bubble and the bubble could not be transported spontaneously and directionally along the track.

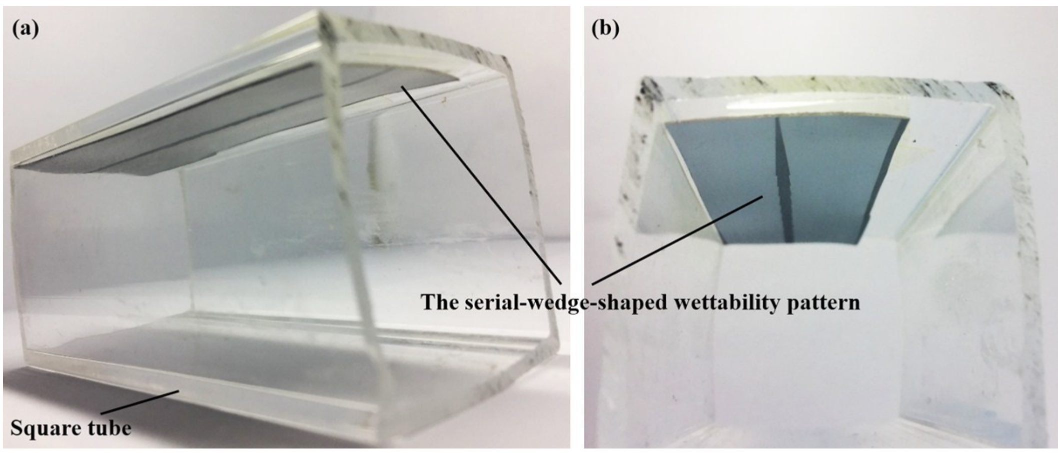

Fig. S7 The digital photos of a square tube whose top wall surface was fixed with a serial-wedge-shaped wettability pattern. (a) and (b) were taken from different optic angle.

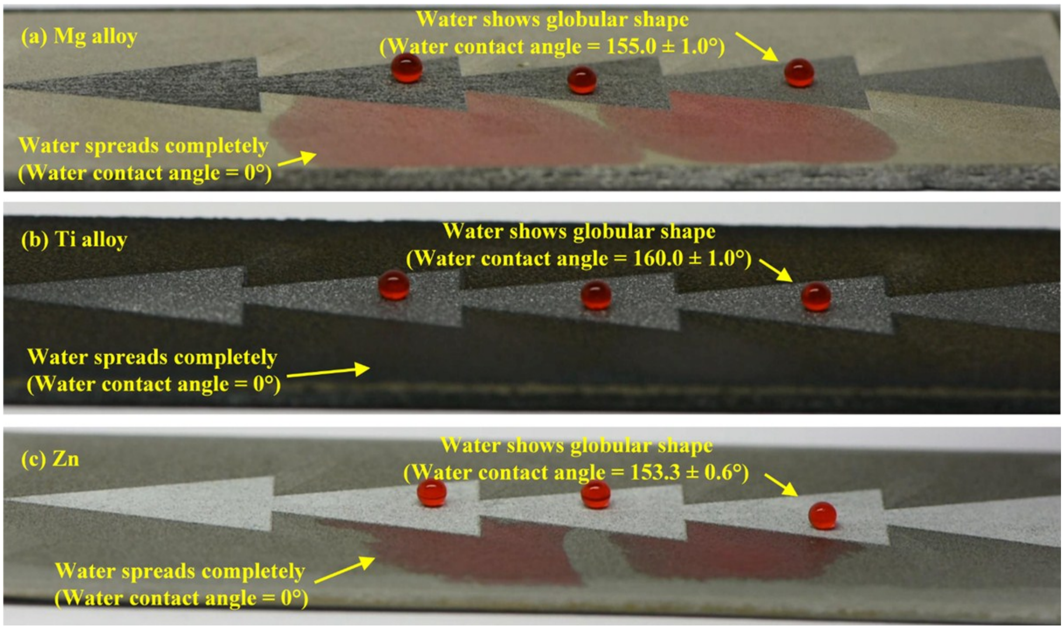

Fig. S8 The serial-wedge-shaped wettability pattern was fabricated on (a) Mg alloy substrate, (b) Ti alloy substrate, and (c) Zn substrate by electrochemical etching and laser etching. The inside interior serial-wedge-shaped region shows superhydrophobic in air and superaerophilic under water. The exterior surrounding region shows superhydrophilic in air and superaerophobic under water.

Video S1

The status of water droplets with volume of 5 μL on the different region of the serial-wedge-shaped wettability pattern. The water droplet in air shows a globular shape with CA of 159±2 ° on the superhydrophobic region but spreads completely with CA of 0 ° on the superhydrophilic region.

Video S2

The top-view transportation processes of a subaqueous gas bubble with volume of 40 μL on the serial-wedge-shaped wettability surface with α=4 °, w_1=0.4 mm, and w_2=2 mm. Gas bubble transported first but then stopped and stayed at the first junction.

Video S3

The side-view transportation processes of a subaqueous gas bubble with volume of 40 μL on the horizontal and straight rectangle wettability pattern with a constant width of 2 mm. Owing to the lack of geometric gradient of the rectangle wettability pattern, the bubble could not be transported spontaneously and directionally along the track.

Video S4

The top-view transportation processes of a subaqueous gas bubble with volume of 40 μL on the horizontal and straight serial-wedge-shaped wettability pattern with α=4 °, w_1=1.6 mm, and w_2=2 mm. It is easy for a gas bubble to cross 10 junctions and achieve the transportation distance with 80 mm. The serial-wedge-shaped wettability pattern is straight but it looks a bit bent because of the presence of light refraction.

Video S5

The side-view transportation processes of a subaqueous gas bubble with volume of 40 μL on the horizontal and straight serial-wedge-shaped wettability pattern with α=4 °, w_1=1.6 mm, and w_2=2 mm. It is easy for a gas bubble to cross 10 junctions and achieve the transportation distance with 80 mm. Video is shown at 1/40× speed.

Video S6

The transportation processes of a subaqueous gas bubble with volume of 40 μL on the horizontal and spiral-shaped serial-wedge-shaped wettability pattern with α=4 °, w_1=1.6 mm, and w_2=2 mm. Video is shown at 1/40× speed.

Video S7

The transportation processes of gas jet with flux of 25 mL min^{-1} on the serial-wedge-shaped wettability pattern with α=4 °, w_1=2.6 mm, and w_2=3 mm. All gas bubbles were captured and transported.

Video S8

The transportation processes of a subaqueous gas bubble with volume of 40 μL on the tilted serial-wedge-shaped wettability pattern with α=4 °, w_1=1.6 mm, and w_2=2 mm. The downhill titled angle is about -5 °. The serial-wedge-shaped wettability pattern shows the capacity of anti-buoyancy long-distance SDPT of subaqueous gas bubbles.

Video 9

The transportation processes of a subaqueous gas bubble with volume of 40 μL on the spatial wave-shaped serial-wedge-shaped wettability pattern with α=4 °, w_1=1.6 mm, and w_2=2 mm. The downhill titled angle is about -5 °.

Video S10

The transportation processes of subaqueous gas bubbles on the serial-wedge-shaped wettability pattern (α=4 °, w_1=1.6 mm, and w_2=2 mm) which was fixed on the top wall surface of a square tube with face down.

Video S11

The transportation processes of subaqueous dichloromethane droplets with volume of 20 μL on the serial-wedge-shaped wettability pattern with α=4 °, w_1=1.6 mm, and w_2=2 mm. The serial-wedge-shaped wettability pattern can realize the long-distance SDPT of organic liquid under water.

Video S12

The transportation processes of water droplets in air with volume of 20 μL on the serial-wedge-shaped wettability pattern with α=4 °, w_1=1.6 mm, and w_2=2 mm. The serial-wedge-shaped wettability pattern can realize the long-distance SDPT of water droplets in air.

Video S13

The status of water droplets with volume of 5 μL on the different region of the serial-wedge-shaped wettability pattern on Mg alloy substrate, Ti alloy substrate, and Zn substrate.